

# Fraction of the X-ray selected AGNs with optical emission lines in galaxy groups

Feng Li<sup>1,2</sup>, Qirong Yuan<sup>1</sup>, Weihao Bian<sup>1</sup>, Xi Chen<sup>1</sup>, Pengfei Yan<sup>3</sup>

## Abstract

Compared with numerous X-ray dominant active galactic nuclei (AGNs) without emission-line signatures in their optical spectra, the X-ray selected AGNs with optical emission lines are probably still in the high-accretion phase of black hole growth. This paper presents an investigation on the fraction of these X-ray detected AGNs with optical emission-line spectra in 198 galaxy groups at  $z < 1$  in a rest frame 0.1-2.4 keV luminosity range  $41.3 < \log(L_X/\text{erg s}^{-1}) < 44.1$  within the Cosmological Evolution Survey (COSMOS) field, as well as its variations with redshift and group richness. For various selection criteria of member galaxies, the numbers of galaxies and the AGNs with optical emission lines in each galaxy group are obtained. It is found that, in total 198 X-ray groups, there are 27 AGNs detected in 26 groups. AGN fraction is on average less than  $4.6(\pm 1.2)\%$  for individual groups hosting at least one AGN. The corrected overall AGN fraction for whole group sample is less than  $0.98(\pm 0.11)\%$ . The normalized locations of group AGNs show that 15 AGNs are found to be located in group centers, including all 6 low-luminosity group AGNs ( $L_{0.5-2\text{keV}} < 10^{42.5}\text{erg s}^{-1}$ ). A weak rising tendency with  $z$  are found: overall AGN fraction is 0.30-0.43% for the groups at  $z < 0.5$ , and 0.55-0.64% at  $0.5 < z < 1.0$ . For the X-ray groups at  $z > 0.5$ , most member AGNs are X-ray bright, optically dull, which results in a lower AGN fractions at higher redshifts. The AGN fraction in isolated fields also exhibits a rising trend with redshift, and the slope is consistent with that in groups. The environment of galaxy

groups seems to make no difference in detection probability of the AGNs with emission lines. Additionally, a larger AGN fractions are found in poorer groups, which implies that the AGNs in poorer groups might still be in the high-accretion phase, whereas the AGN population in rich clusters is mostly in the low-accretion, X-ray dominant phase.

**Keywords** galaxies: active – galaxies: nuclei – galaxies: groups – galaxies: field – quasars: emission lines

## 1 Introduction

It is believed that Active galactic nuclei (AGNs) are powered by the accretion around the central supermassive black holes (SMBHs). The trigger mechanism of such nuclear activity is still subject to debate. The co-evolution between the growth of SMBHs and the formation of stars in galaxies suggests that processes to trigger star formation also trigger SMBHs accretion in AGNs (e.g., Boyle et al. 1998; Franceschini et al. 1999; Ferrarese & Merritt 2000; Gebhardt et al. 2000; Tremaine et al. 2002; Merloni et al. 2004; Silverman et al. 2008; Martini et al. 2009, 2013; Kormendy & Ho 2013). It is possible that SMBHs accretion in luminous AGNs are triggered by major mergers of gas-rich galaxies (e.g., Kauffmann & Haehnelt 2000; Sanders et al. 1988; Barnes & Hernquist 1991; Hopkins et al. 2006; Hopkins & Quataert 2011), which is supported by the small-scale excess of quasar-quasar and quasar-galaxy pairs (Hennawi et al. 2006; Serber et al. 2006). For less luminous AGNs, some other mechanisms, such as minor mergers, large-scale bars, disk instabilities, turbulence in the interstellar medium (ISM), have also been proposed to fuel star formation and SMBH growth at lower rates (e.g., Simkin et al. 1980; Elmegreen et al. 1998; Genzel et al. 2008; Hopkins & Quataert 2010, 2011).

Feng Li, Qirong Yuan, Weihao Bian, Xi Chen, Pengfei Yan

<sup>1</sup>Department of Physics and Institute of Theoretical Physics, Nanjing Normal University, Nanjing 210023, China

<sup>2</sup>School of Mathematics and Physics, Changzhou University, Changzhou 213164, China

<sup>3</sup>School of Mathematics and Physics, Qingdao University of Science and Technology, Qingdao 266061, China

Groups of galaxies are supposed to be an ideal environment for such gas-fueling mergers due to their high galaxy densities and low velocity dispersions. However, for the denser environment, i.e., rich clusters of galaxies, their hotter intracluster media (ICM) and larger velocity dispersions may drive some additional processes to impact the cold gas fueling of the SMBHs (e.g., Miyaji et al. 2011; Bekki 2014; Boselli et al. 2014; Koulouridis et al. 2014; Vijayaraghavan & Ricker 2015; Peng et al. 2015). These processes include the removal of cold gas via ram pressure stripping, evaporation of galactic gas by the hot ICM, tidal effects due to the cluster potential, and gas starvation due to the absence of new infall of cold gas.

The AGN fraction in galaxy groups/clusters provides valuable additional observational constraints on AGN fueling mechanisms and the growth of the central SMBHs, as well as the impact of AGNs on the intracluster medium (ICM) over cosmic time (e.g., Martini et al. 2009). Nearly complete absence of quasars in rich clusters can be interpreted by the relative lack of cold gas and major mergers (Barnes & Hernquist 1992). Investigation on fraction of the AGNs with optical emission lines selected from the Sloan Digital Sky Survey (SDSS) show that luminous AGNs are rarer in denser environments (Kauffmann et al. 2004), while the fraction of low-luminosity AGNs in SDSS and radio observations does not decrease remarkably in richer clusters (Miller et al. 2003; Best et al. 2005; Martini et al. 2006).

Based on different AGN selection methods, such as optical spectra, X-ray luminosity, mid-infrared color index and radio luminosity, the AGN fraction within groups/clusters has been extensively studied, as well as observational properties of AGNs in groups/clusters (e.g., Dressler et al. 1985; Martini et al. 2006, 2007; Eastman et al. 2007; Martini et al. 2009; Haggard et al. 2010; Tomczak et al. 2011; Martini et al. 2013; Oh et al. 2014; Tzanavaris et al. 2014). For a very nearby sample of 1095 galaxies in rich clusters and 173 field galaxies with optical spectra, Dressler et al. (1985) found that 1% of cluster galaxies host AGNs, while 5% of field galaxies do. With a spectroscopic survey of X-ray point sources in eight low-redshift clusters of galaxies with  $0.05 < z < 0.31$ , Martini et al. (2006) estimated that the fraction of cluster galaxies with  $M_R < -20$  mag which host the AGNs with  $L_X > 10^{41} \text{erg s}^{-1}$  is  $\sim 5\%$ . For 32 galaxy clusters with  $0.05 < z < 1.3$ , Martini et al. (2009) found the AGN fraction is 0.134% in low- $z$  clusters ( $z < 0.4$ ), and increase significantly to 1% in high- $z$  clusters ( $z > 0.4$ ) (also see Eastman et al. 2007). For a sample of 13 clusters of galaxies at higher redshifts (i.e.,  $1 < z < 1.5$ ), Martini et al. (2013) found

that the AGN fraction in clusters is  $3.0^{+2.4}_{-1.4}\%$ , suggesting the rising tendency of AGN fraction in clusters with redshift from 0.05 to 1.5. With the *Chandra* Multi-wavelength Project (ChAMP) and SDSS data, using  $L_{0.5-8\text{keV}} > 10^{42} \text{erg s}^{-1}$  to select AGNs, Haggard et al. (2010) found that the AGN fraction in groups is 0.16% for  $z \leq 0.125$ , and 3.8% for  $z \leq 0.7$ , depending on the selection criteria of field galaxies (also see Martini et al. 2009). For a mass-selected sample of galaxies from the 10k catalog of the zCOSMOS spectroscopic redshift survey, Silverman et al. (2009) identified 147 AGNs, and found no significant difference of AGN fraction in groups with that in fields.

Compared with optically selected AGNs, the AGNs revealed by *Chandra* and *XMM-Newton* surveys have a higher spatial number density that peaks at low redshift (Hasinger et al. 2005), and show a stronger spatial clustering (Yang et al. 2006). The fraction of X-ray selected AGNs in clusters is significantly higher than that of the optically selected AGNs with emission lines (e.g. Martini et al. 2009). Large number of X-ray AGNs in clusters show little or no optical AGN signatures (Martini et al. 2006). Shen et al. (2007) studied the AGN population in eight low-redshift poor groups of galaxies, and found that the X-ray bright, optically dull AGNs are entirely absent from the less dynamically evolved groups, which supports a scenario for AGN accretion evolution: AGN activity is initially triggered by galaxy merging, leading to a high accretion rate and an optically dominant phase. With the decline of accretion rate, the AGN gradually enters into an X-ray dominant phase without optical emission lines. Thus the optically and X-ray selected AGNs harbor the same population of SMBHs observed at different epochs. According to this picture, the majority of AGNs in poor galaxy groups are likely in the high-accretion phase with optical emission signatures, and the early phase of accretion evolution should be more sensitive to the ideal environment of gas-fueling mergers — groups of galaxies.

In this paper, we plan to take a large sample of X-ray selected galaxy groups in the COSMOS field to investigate the fraction of X-ray selected AGNs with optical emission lines which might be in the high-accretion phase. This investigation will focus on cosmological evolution and richness dependence of the AGN fraction in the redshift region  $z < 1$ . §2 describes the data and samples. The AGN fractions in groups and in fields are given in §3, as well as its cosmological evolution and variation with group richness. The main conclusions are given in §4. Throughout this work we assume a standard  $\Lambda$ CDM cosmology with  $\Omega_\Lambda = 0.7$ ,  $\Omega_M = 0.3$  and  $H_0 = 70 \text{ km s}^{-1} \text{ Mpc}^{-1}$ .

## 2 Data and sample

### 2.1 Galaxy groups in COSMOS

The COSMOS field covers about  $2 \text{ deg}^2$  equatorial area in the constellation *Sextans*. It has been photometrically observed in a broad range of wavelengths (over 30 bands from the ultraviolet, optical, and infrared), and it also has been mapped through 54 overlapping *XMM-Newton* pointing and additional *Chandra* observations for the central  $0.9 \text{ deg}^2$  region (e.g. Hasinger et al. 2007; Finoguenov et al. 2007; Ilbert et al. 2009; Brusa et al. 2010). Group catalogs have been constructed in this field on the basis of X-ray data (e.g., Finoguenov et al. 2007; George et al. 2011), zCOSMOS spectroscopy (e.g., Knobel et al. 2009), and photometric redshifts (Gillis & Hudson 2011).

In this paper we will take the group catalog given by George et al. (2011), including 211 extended X-ray selected galaxy groups ( $0 < z < 1$ ) in a rest-frame  $0.1\text{--}2.4 \text{ keV}$  luminosity range of  $41.3 < \log(L_X/\text{erg s}^{-1}) < 44.1$  in the COSMOS field, among which 165 groups have reliable optical counterparts (Finoguenov et al. 2007, 2010)<sup>1</sup>. Using a restrict Bayesian algorithm, George et al. (2011) assigned 115,844 galaxies to groups based on precise photometric redshifts (Ilbert et al. 2009; Allevalo et al. 2012). These galaxies satisfy  $z_{ph} < 1.2$  and  $I(F814W) < 24.2 \text{ mag}$ , and require a  $3\sigma$  detection in the  $K_s$  band for the stellar mass estimation, which is complete to a typical depth of  $K_s = 24$ . With  $L_X - M$  scaling relation calibrated by weak gravitational lensing, the halo masses  $M_{200}$  are calculated in the range  $10^{13} \leq M_{200}/M_\odot \leq 10^{14}$  for these galaxy groups within  $R_{200}$ , where  $M_{200} \equiv M(< R_{200}) = 200\rho_c(z)\frac{4}{3}\pi R_{200}^3$ , and  $R_{200}$  is the radius at which the mean interior density is equal to 200 times the critical density (Leauthaud et al. 2010). Roughly 20% of group members have spectroscopic redshifts.

The membership probability for each galaxy in groups,  $P_{\text{mem}}$ , is given by George et al. (2011). With a spectroscopic subsample, George et al. (2011) estimated the purity ( $p$ ) and completeness ( $c$ ) for different membership probability thresholds. For a threshold of  $P_{\text{mem}} > 0.1$ , the purity and completeness of member selection are about 63% and 97%, respectively. With a higher threshold of  $P_{\text{mem}}$ , the purity is improved, and the completeness is deteriorated. For  $P_{\text{mem}} > 0.3$ ,  $p = 67\%$  and  $c = 94\%$ . For  $P_{\text{mem}} > 0.5$ ,  $p = 69\%$  and  $c = 92\%$ . Taking the threshold of  $P_{\text{mem}} > 0.1$ , there are 198 X-ray selected groups with  $z < 1.0$  in the COSMOS field.

### 2.2 X-ray selected AGNs with emission lines

Entire COSMOS field ( $2 \text{ deg}^2$ ) has been mapped by the *XMM-Newton* pointing observations ( $\sim 1.55 \text{ Ms}$ ), and only the central region ( $0.9 \text{ deg}^2$ ) is covered by the *Chandra* observations with a higher spatial resolution (Finoguenov et al. 2007; Brusa et al. 2010). With the *XMM-Newton* survey of the COSMOS field, there are 1,848 point-like sources detected, at least one of the soft ( $0.5\text{--}2 \text{ keV}$ ), hard ( $2\text{--}10 \text{ keV}$ ) and ultra-hard ( $5\text{--}10 \text{ keV}$ ) bands down to limiting fluxes of  $5 \times 10^{-16}$ ,  $3 \times 10^{-15}$ , and  $7 \times 10^{-15} \text{ erg cm}^{-2} \text{ s}^{-1}$ , respectively. Only about half sources are detected with the *Chandra*.

To match the sample of 198 X-ray selected groups with  $z < 1$ , we need to construct a contiguous ( $2 \text{ deg}^2$ ) X-ray selected AGN sample, with well-defined flux limits and a reliable estimate of spectroscopic completeness. In this paper we will take the AGN sample obtained from the medium-depth ( $\sim 60 \text{ ks}$ ) *XMM-COSMOS* survey. Brusa et al. (2010) matched a multi-wavelength counterpart to 1,797/1,848 sources<sup>2</sup>. There are 730 AGNs identified by a lot of good-quality spectroscopic follow-up programs of XMM point sources, such as Magellan/IMACS and MMT observation campaigns, and VIMOS/zCOSMOS bright and faint projects (e.g. Gilli et al. 2009). The objects having at least one broad optical emission line (FWHM  $> 2000 \text{ km s}^{-1}$ ) are classified as broad-line AGNs. Those with unresolved high-ionization lines, or exhibiting line ratios indicating AGN activity in the BPT diagram (Baldwin et al. 1981) are classified as narrow-line AGNs. For the remaining objects whose spectral range does not allow to construct line diagnostics, the objects with rest-frame hard X-ray luminosities in excess than  $2 \times 10^{42} \text{ erg s}^{-1}$  are also classified as narrow-line AGNs (see section 5.1 in Brusa et al. 2010). The majority (403,  $\sim 55\%$ ) are broad-line AGNs, whereas the rest AGNs are narrow-line ones. Majority of broad-line AGNs are observed at  $z > 1.0$  and with  $0.2\text{--}2 \text{ keV}$  X-ray luminosities  $\log(L_X > 41.5 \text{ erg s}^{-1})$ , while narrow-line AGNs are observed down to very low X-ray luminosities (see Figure 2 in Gilli et al. 2009). Gilli et al. (2009) studied the spatial clustering the X-ray selected AGNs in the XMM-Newton field, based on an analysis of the sample of 538 X-ray selected AGNs with  $I_{\text{AB}} < 23$  and  $0.2 < z < 3.0$ . They estimated the spectroscopic completeness is about 60% for  $z < 1.2$  and the spectroscopic selection does not include any bias against high-redshift objects. Following Gilli et al. (2009), we take  $I_{\text{AB}} < 23$  and  $z < 1.0$ , 338 out of 730 AGNs ( $\sim 46.3\%$ ) are selected to have optical emission line signatures. This

<sup>1</sup><http://irsa.ipac.caltech.edu/data/COSMOS/tables/groups/>

<sup>2</sup><http://vizier.cfa.harvard.edu/viz-bin/VizieR?source=J/ApJ/716/348>

spectroscopic completeness ( $\sim 60\%$ ) will be adopted in our further estimate of AGN fraction.

### 2.3 AGNs/galaxies in groups and fields

Given a threshold of the membership probability  $P_{\text{mem}}$ , the member galaxies for each group are obtained. Then we cross-identify above AGN sample with the member galaxies. With  $P_{\text{mem}} > 0.1$ , there are 27 AGNs in 26 groups with 6,597 member galaxies (see Table 1), and their distributions of membership probabilities,  $P_{\text{mem}}$  are shown in Fig. 1. For these 27 AGNs in 26 galaxy groups, the AGN membership probability ( $P_{\text{mem}}$ ) are large than 0.5, with a peak in the range of  $0.8 < P_{\text{mem}} < 0.9$ . The 27 AGNs in groups are nearly all narrow-line AGNs, except one broad-line AGN, which can be interpreted by the fact that the broad-line AGNs are on average high-luminosity AGNs at  $z > 1$ . For selecting field galaxies with  $z < 1$ , we take  $P_{\text{mem}} = 0$  and GROUP\_FLAG = -1, and obtain 74,350 field galaxies, including 299 AGNs with emission lines.

In order to avoid the selection effect on membership assignment, we adopt three membership probability thresholds (i.e. 0.1, 0.3 and 0.5), and obtain three samples of member galaxies/AGNs in groups, respectively. Table 1 shows the statistics of 27 AGNs in 26 groups and galaxies in all 198 groups for three  $P_{\text{mem}}$  thresholds, including purity, completeness, number of member galaxies and AGNs, and the overall mean AGN fraction in all 198 groups. The distributions of membership probability ( $P_{\text{mem}}$ ) for 27 AGNs and galaxies in all 198 groups are shown in Fig. 1. The redshift distributions for three samples of group members are shown in Fig. 2. It is found that the peak redshift of group galaxies appears in the range of  $0.3 < z < 0.4$  (see Fig. 2). As  $P_{\text{mem}}$  threshold increases, the number of member galaxies decreases, but the distribution with photometric redshifts ( $z_{\text{phot}}$ ) remains unchanged. The Kolmogorov-Smirnov tests show that three  $z_{\text{phot}}$  distributions obey the same distribution with the probabilities more than 86%.

## 3 AGN fraction in groups and fields

### 3.1 The AGN fraction in each group

From 198 X-ray selected groups ( $z < 1.0$ ,  $P_{\text{mem}} > 0.1$ ) in the COSMOS field, it is found that there are 27 AGNs appearing in 26 groups. The AGN fraction for a given group is defined as  $f_{\text{AGN}}^{\text{group}} = N_{\text{AGN}}^{\text{group}}/N_{\text{gal}}^{\text{group}}$ , where  $N_{\text{AGN}}^{\text{group}}$  and  $N_{\text{gal}}^{\text{group}}$  are the numbers of AGNs and galaxies in a group, respectively. We calculate the

AGN fractions in these 26 groups, as well as their errors. We estimate  $1 \sigma$  errors based on a Poisson distribution due to the small number of objects in each group (Silverman et al. 2008). Considering the purity ( $p$ ) and completeness ( $c$ ), the AGN fraction ( $f_{\text{AGN}}^{\text{group}}$ ) keeps unchanged, the corresponding error will be magnified by  $\sqrt{c/p}$ . Fig. 3 shows the the AGN fraction in each group as a function of spectroscopic redshifts for these 26 groups. The Pearson correlation coefficient ( $r_s$ ), and the slope ( $\Delta f_{\text{AGN}}^{\text{group}}/\Delta z$ ) of the linear fitting are also presented. It can be seen that, for three samples,  $f_{\text{AGN}}^{\text{group}}$  has a very weak rising trend with redshift, and the linear correlations are very weak. For quantifying the distribution of AGN fractions in groups, we apply the ROSTAT software (Beers et al. 1990) to calculate the biweight location, which is analogous to the mean value. The biweight locations of AGN fraction for three samples are  $3.5(\pm 0.6)\%$ ,  $4.5(\pm 0.9)\%$ ,  $4.6(\pm 1.2)\%$ , respectively, suggesting that the average AGN fraction in X-ray groups at  $z < 1$  is less than 5% for individual groups.

It should be noted that, for more than 87% of X-ray groups, none of member galaxies has been spectroscopically identified as AGNs. Table 1 shows the overall mean AGN fraction for three samples. For larger probability threshold, number of group galaxies is smaller, and the AGN number remain the same, resulting in larger overall mean AGN fraction,  $\langle f_{\text{AGN}} \rangle$ , from 0.41% to 0.59%. Considering the spectroscopic completeness of about 60% (Gilli et al. 2009), the mean AGN fraction can be corrected for each sample. The corrected mean AGN fractions,  $\langle f_{\text{AGN}}^{\text{corr}} \rangle$ , are listed in Table 1. Conservatively, for 198 X-ray selected groups at  $z < 1$ , overall fraction of the AGNs with emission lines is less than 1 %.

### 3.2 Location of 27 AGNs in 26 galaxy groups

It is hard to investigate the distribution of X-ray luminous AGNs within individual groups/clusters due to the rarity of luminous AGNs and large uncertainties of photometric redshifts. Fig. 4 shows normalized projected distance to the most massive galaxy in each group,  $R/R_{200}$ , of 27 AGNs versus spectroscopic redshifts and the rest-frame soft X-ray luminosity (0.5–2 keV). There are 15 out of 27 AGNs with  $R/R_{200} = 0$ , suggesting that they are all the most massive group galaxies. For the groups at  $z < 0.5$ , 9 out of 10 AGNs are located at group center (i.e.,  $R/R_{200} = 0$ ). For the groups at  $z > 0.5$ , some emission-line AGNs are located in outer region of groups, up to  $\sim 0.9R_{200}$ . There are 21 out of 27 AGNs with  $L_{\text{X},0.5-2\text{keV}} > 10^{42.5} \text{ erg s}^{-1}$ , indicating that majority of the group AGNs are X-ray luminous

**Table 1** Statistics for three samples of member galaxies/AGNs in groups.

No. of Samples	$P_{\text{mem}}$ Threshold	Number of Groups	Number of AGNs	Number of Galaxies	Purity ( $p$ )	Completeness ( $c$ )	$\langle f_{\text{AGN}} \rangle$ (%)	$\langle f_{\text{AGN}}^{\text{corr}} \rangle$ (%)
1	0.1	26	27	6597	0.63	0.97	$0.41 \pm 0.08$	$0.68 \pm 0.08$
2	0.3	26	27	5617	0.67	0.94	$0.48 \pm 0.09$	$0.80 \pm 0.09$
3	0.5	26	27	4606	0.69	0.92	$0.59 \pm 0.11$	$0.98 \pm 0.11$

galaxies. It is interesting to see that all 6 faint group AGNs with  $L_{\text{X},0.5-2\text{keV}} < 10^{42.5} \text{ erg s}^{-1}$  are found to be located at group centers. The low-luminosity AGNs seems to have higher probabilities to be found at the centers of low- $z$  groups of galaxies.

### 3.3 Cosmological evolution of overall AGN fraction

For  $P_{\text{mem}} > 0.1$ , there are 26 X-ray selected groups at  $z < 1$  hosting at least one AGN with emission lines. For the rest of groups, no galaxies are found to be in the high-accretion AGN phase. The groups with no detection of emission-line AGNs should be taken into account when we evaluate the overall AGN fraction in groups. In order to investigate cosmological evolution of overall AGN fraction in groups, the sample of 198 X-ray groups are divided into 10  $z$ -bins with a interval width of  $\Delta z = 0.1$ . Considering the spectroscopy completeness, we calculate the overall AGN fraction in groups for each  $z$ -bin,  $f_{\text{AGN}}^{\text{corr}} = N_{\text{AGN}} / (0.6N_{\text{gal}})$ , where  $N_{\text{AGN}}$  and  $N_{\text{gal}}$  are the number of emission-line AGNs and galaxies in groups for each  $z$ -bin, respectively. Due to small number of objects in each  $z$ -bin,  $1 \sigma$  errors of number counts are estimated on the basis of a Poisson distribution (Silverman et al. 2008). The error of overall AGN fraction in each  $z$ -bin can be derived by error-propagation, and considering a magnifying factor of  $\sqrt{c/p}$ . As illustrated in Fig. 5, overall AGN fraction ( $f_{\text{AGN}}^{\text{corr}}$ ) is found to have a slight rising trend with redshift, and their Spearman correlation coefficients,  $r_s$ , are in a range from 0.36 to 0.39 for three samples. The rising tendency for overall AGN fraction is basically consistent with the results in Martini et al. (2009) and Oh et al. (2014).

Because of small number of group AGNs with emission lines, the tendency of overall AGN fraction is rather uncertain for the binning strategy of  $\Delta z = 0.1$ . For decreasing uncertainties in AGN fraction estimates, we split samples into low- $z$  ( $z < 0.5$ ) and high- $z$  ( $0.5 < z < 1.0$ ) subsamples. For sample 1 ( $P_{\text{mem}} > 0.1$ ), overall AGN fractions are  $0.30(\pm 0.11)\%$  and  $0.55(\pm 0.17)\%$  for low- and high- $z$  bins, respectively. For sample 2 ( $P_{\text{mem}} > 0.3$ ), they are  $0.35(\pm 0.13)\%$  and  $0.64(\pm 0.19)\%$  respectively for low- and high- $z$  subsamples. For sample 3 ( $P_{\text{mem}} > 0.5$ ), overall AGN fractions

are  $0.43(\pm 0.15)\%$  and  $0.64(\pm 0.19)\%$ . In sum, the overall AGN fraction in groups is  $0.30\text{-}0.43\%$  at  $z < 0.5$ , and it is  $0.55\text{-}0.64\%$  at  $0.5 < z < 1.0$ .

Considerable efforts have been made to measure the AGN fraction with redshifts in groups and clusters. Eastman et al. (2007) was the first to report a significant increase of AGN fraction in galaxy clusters with two luminosity thresholds ( $L_{\text{X,H}} > 10^{42} \text{ erg s}^{-1}$  and  $L_{\text{X,H}} > 10^{43} \text{ erg s}^{-1}$ ) from  $z \sim 0.2$  to  $z \sim 0.6$ . Martini et al. (2009) also obtained a significant increase of AGN fraction for 32 galaxy clusters with  $0.05 < z < 1.3$ , finding the AGN fractions are  $0.134\%$  in low- $z$  clusters ( $z < 0.4$ ) and  $1.00\%$  in high- $z$  clusters ( $z > 0.4$ ), respectively. Taking  $L_{\text{X},0.5-8\text{keV}} > 10^{42} \text{ erg s}^{-1}$  to select AGNs, Haggard et al. (2010) found that the AGN fraction in groups is  $0.16(\pm 0.06)\%$  for  $z \leq 0.125$ , and  $3.8(\pm 0.92)\%$  for  $z \leq 0.7$ . Using three different selection techniques (mid-IR color, radio luminosity, and X-ray luminosity), Galametz et al. (2009) extended this rising trend with redshift up to  $z \sim 1.5$ , and the observed increase with redshift is more pronounced in the galaxy cluster than in the field (see Galametz et al. 2009, Figure 2). Our result also presents an increasing trend of the fraction of emission-line AGNs with redshift, which is in accordance with most previous studies. This suggests the evolution of AGN population in rich clusters has a Butcher-Oemler effect similar to star forming galaxies (Butcher & Oemler 1984). It should be noted that the significant variations in AGN fraction estimate among previous works are mainly due to different selection criteria of the samples of AGNs and cluster galaxies, which result in somewhat different redshift distributions and limiting magnitudes for the samples under comparison.

For observing the probable environmental effect on AGN fraction, we investigate the AGN fraction in fields. We select the member AGNs/galaxies in groups and in fields by setting  $P_{\text{mem}} > 0$  and  $P_{\text{mem}} = 0$ , respectively. The statistics of galaxies/AGNs in groups and isolated fields is presented in Table 2. The overall AGN fractions in 10  $z$ -bins (i.e.,  $\Delta z = 0.1$ ) are calculated. The AGN fractions in groups and fields as a function of  $z$  are shown in Fig. 6. We find that there is a strong correlation between the field AGN fraction and  $z$  with a Spearman correlation coefficient of  $r_s = 0.945$ . For the

**Table 2** Statistics for galaxies and AGNs in all 198 groups ( $P_{\text{mem}} > 0$ ) and in fields ( $P_{\text{mem}} = 0$ )

redshift Range	Number of all AGNs	Number of group AGNs	Number of field AGNs	Number of group galaxies	Number of field galaxies	$f_{\text{AGN}}^{\text{corr}}$ (%) in group	$f_{\text{AGN}}^{\text{corr}}$ (%) in field
(0.0, 0.1)	3	0	3	232	1514	0	$0.33 \pm 0.11$
[0.1, 0.2)	12	5	7	845	3149	$0.99 \pm 0.27$	$0.37 \pm 0.08$
[0.2, 0.3)	12	1	11	1228	4975	$0.14 \pm 0.08$	$0.37 \pm 0.07$
[0.3, 0.4)	41	7	34	1903	9235	$0.61 \pm 0.14$	$0.61 \pm 0.06$
[0.4, 0.5)	21	1	20	782	7574	$0.21 \pm 0.13$	$0.44 \pm 0.06$
[0.5, 0.6)	27	3	24	521	7239	$0.96 \pm 0.33$	$0.55 \pm 0.07$
[0.6, 0.7)	48	5	43	836	10311	$1.00 \pm 0.27$	$0.70 \pm 0.06$
[0.7, 0.8)	49	4	45	898	9975	$0.74 \pm 0.22$	$0.75 \pm 0.07$
[0.8, 0.9)	60	4	56	753	10239	$0.89 \pm 0.27$	$0.91 \pm 0.07$
[0.9, 1.0)	58	2	56	578	10139	$0.58 \pm 0.25$	$0.92 \pm 0.07$

corrected AGN fraction in groups, the correlation coefficient  $r_s = 0.461$ , which is larger than those for stricter membership selections shown in Fig. 5. The AGN fraction in isolated fields also exhibits a rising trend with  $z$ , and the slope is consistent with that in groups. The environment in galaxy groups seems to have no obvious influence on detection probability of the AGNs with emission features, indicating that the physical process concerning AGN fueling seems to be insensitive to the group environment. At  $z > 0.7$ , the difference of AGN fraction between high- and low-density environments is negligible, which is consistent with the result in Martini et al. (2013) that the X-ray AGN fractions in the field and clusters are similar at  $1 < z < 1.5$ . However, Kauffmann et al. (2004) found that fraction of the local AGNs with strong [O III] emission decreases with local density, and twice as many AGNs are found in low-density regions as in high.

### 3.4 AGN fraction as a function of group richness

To analyze how AGN fractions vary with group richness, the samples of group galaxies/AGNs selected by  $P_{\text{mem}} > 0$ , are split into three  $z$ -bins (say,  $z \leq 0.4$ ,  $0.4 < z \leq 0.7$ , and  $0.7 < z < 1.0$ ) and into three bins of group richness (say,  $N \leq 30$ ,  $30 < N \leq 50$ , and  $N > 50$ ). In Fig. 7 we can see that the corrected AGN fractions show a clear decreasing trend with richness for all three redshift bins. The error bars of redshift represent the median absolute deviation from the median redshift in each  $z$ -bin. We find a larger fraction of emission-line AGNs in poor groups ( $N \leq 30$ ), supporting the view that galaxies in groups retain larger reservoirs of cold gas to fuel AGN activity than their counterparts in clusters (e.g. Shen et al. 2007; Georgakakis et al. 2008; Arnold et al. 2009; Martini et al. 2009; Allevato et al. 2012). Tzanavaris et al. (2014) studied *Chandra* X-ray point source catalogs for 9 Hickson Compact Groups

(HCGs) at a median redshift  $z_{\text{med}} = 0.03$ , and concluded that the AGN fraction in groups is higher than that in clusters. In stark contrast to the above conclusion, some authors yielded the percentage of AGN in clusters is similar as that in fields while using different AGN selection criteria (e.g. Haggard et al. 2010; Klesman & Sarajedini 2012; Martini et al. 2013).

A larger fraction of the AGNs with strong emission lines in poor groups suggests that the density environment may not only influence on the fueling mechanisms but also on the evolution of galaxies. Majority of the AGNs in poor groups are probably in the high-accretion optically dominant phase, whereas the AGN population in rich clusters is mostly in the low-accretion X-ray dominant phase. This finding is in accordance with the scenario of AGN accretion evolution that was proposed by Shen et al. (2007).

## 4 Conclusions

Based on a sample of 198 X-ray galaxy groups in a rest frame 0.1-2.4 keV luminosity range  $41.3 < \log(L_X/\text{erg s}^{-1}) < 44.1$  and a sample of the spectroscopically confirmed AGNs in the XMM-COSMOS survey, we investigate the fractions of the AGNs with emission lines in galaxy groups at  $z < 1$ , as well as the variations with redshift and group richness. The main conclusions can be summarized as follows:

(1) For various selection criteria of member galaxies (i.e.,  $P_{\text{mem}} > 0.1, 0.3, 0.5$ ), merely 27 AGNs with emission lines are found in 26 groups. Taking the AGN fraction estimated for the strictest selection criterium  $P_{\text{mem}} > 0.5$  as the upper limit, the AGN fraction is on average less than  $4.6(\pm 1.2)\%$  for individual groups hosting at least one AGN. The corrected overall AGN fraction for our group sample is less than  $0.98(\pm 0.11)\%$ .

(2) The normalized locations of AGNs show that all group AGNs with 0.5-2 keV luminosities less than  $10^{42.5} \text{erg s}^{-1}$  are found to be located at the centers of groups.

(3) The overall AGN fractions in various  $z$ -bins are estimated, and a weak rising tendency with  $z$  are found. Overall AGN fractions in group are 0.30-0.43% for the groups at  $z < 0.5$ , and 0.55-0.64% at  $0.5 < z < 1.0$ . For X-ray groups at  $z > 0.5$ , most member AGNs are X-ray bright, optically dull, which results in a lower AGN fractions at higher redshifts.

(4) The AGN fraction in isolated fields also exhibits a rising trend with  $z$ , and the slope is consistent with that in groups. The environment of galaxy groups seems to make no difference in detection probability of the AGNs with emission lines.

(5) For the groups in various redshift ranges, a larger AGN fractions are found in poorer groups. For those poor groups with less than 30 member galaxies, a larger fraction of group AGNs might still be in the high-accretion phase, whereas the AGN population in rich clusters is mostly in the low-accretion X-ray-dominant phase.

### **Acknowledgements**

We thank the referee for his/her detailed comments and suggestions. Funding for this work has been provided by the National Natural Science Foundation of China (NSFC) (Nos. 11173016, 11433005) and by the Special Research Fund for the Doctoral Program of Higher Education (grant No. 20133207110006).

## References

- Allevato, V., Finoguenov, A., Hasinger, G., et al. 2012, *Astrophys. J.*, 758, 47
- Arnold, T. J., Martini, P., Mulchaey, J. S., Berti, A., & Jeltama, T. E. 2009, *Astrophys. J.*, 707, 1691
- Baldwin, J. A., Phillips, M. M., & Terlevich, R. 1981, *PASP*, 93, 5
- Barnes, J. E., & Hernquist, L. E. 1991, *Astrophys. J.*, 370, L65
- Barnes, J. E., & Hernquist, L. E. 1992, *Annu. Rev. Astron. Astrophys.*, 30, 705
- Beers, T. C., Flynn, K., & Gebhardt, Karl. 1990, *Astron. J.*, 100, 32
- Bekki, K. 2014, *Mon. Not. R. Astron. Soc.*, 438, 444
- Best, P. N., et al. 2005, *Mon. Not. R. Astron. Soc.*, 362, 9
- Boselli, A., Cortese, L., Boquien, M., et al. 2014, *Astron. Astrophys.*, 564, A67
- Boyle, B. J., Georgantopoulos, I., Blair, A. J., et al. 1998, *Mon. Not. R. Astron. Soc.*, 296, 1
- Brusa, M., Civano, F., Comastri, A., et al. 2010, *Astrophys. J.*, 716, 348
- Butcher, H., Oemler, A., Jr. 1984, *Astrophys. J.*, 285, 426
- Dressler, A., Thompson, I. B., & Shectman, S. A. 1985, *Astrophys. J.*, 288, 481
- Eastman, J., Martini, P., Sivakoff, G., et al. 2007, *Astrophys. J.*, 664, L9
- Elmegreen, B. G., Elmegreen, D. M., Brinks, E., et al. 1998, *Astrophys. J.*, 503, 119
- Ferrarese, L., & Merritt, D. 2000, *Astrophys. J.*, 539, L9
- Finoguenov, A., Guzzo, L., Hasinger, G., et al. 2007, *Astrophys. J. Suppl. Ser.*, 172, 182
- Finoguenov, A., Watson, M. G., Tanaka, M., et al. 2010, *Mon. Not. R. Astron. Soc.*, 403, 2063
- Franceschini, A., Hasinger, G., Miyaji, T. & Malquori, D. 1999, *Mon. Not. R. Astron. Soc.*, 310, L5
- Galametz, A., Stern, D., Eisenhardt, P. R. M., et al. 2009, *Astrophys. J.*, 694, 1039
- Gebhardt, K., Bender, R., Bower, G., et al. 2000, *Astrophys. J.*, 539, L13
- Genzel, R., Burkert, A., Bouché, N., et al. 2008, *Astrophys. J.*, 687, 59
- Georgakakis, A., Gerke, B. F., Nandra, K., et al. 2008, *Mon. Not. R. Astron. Soc.*, 391, 183
- George, M. R., Leauthaud, A., Bundy, K., et al. 2011, *Astrophys. J.*, 742, 125
- Gilli, R.; Zamorani, G.; Miyaji, T.; et al. 2009, *Astron. Astrophys.*, 494, 33
- Gillis, B. R., & Hudson, M. J. 2011, *Mon. Not. R. Astron. Soc.*, 410, 13
- Haggard, D., Green, P. J., Anderson, S. F., et al. 2010, *Astrophys. J.*, 723, 1447
- Hasinger, G., Miyaji, T., & Schmidt, M. 2005, *Astron. Astrophys.*, 441, 417
- Hasinger, G., Cappelluti, N., Brunner, H., et al. 2007, *Astrophys. J. Suppl. Ser.*, 172, 29
- Hennawi, J. F., et al. 2006, *Astron. J.*, 131, 1
- Hopkins, P. F., Hernquist, L., Cox, T. J., et al. 2006, *Astrophys. J. Suppl. Ser.*, 163, 1
- Hopkins, P. F., Quataert, E. 2010, *Mon. Not. R. Astron. Soc.*, 407, 1529
- Hopkins, P. F., Quataert, E. 2011, *Mon. Not. R. Astron. Soc.*, 415, 1027
- Ilbert, O., Capak, P., Salvato, M., et al. 2009, *Astrophys. J.*, 690, 1236
- Kauffmann, G., & Haehnelt, M. 2000, *Mon. Not. R. Astron. Soc.*, 311, 576
- Kauffmann, G., et al. 2004, *Mon. Not. R. Astron. Soc.*, 353, 713
- Klesman, A. J., & Sarajedini, V. L. 2012, *Mon. Not. R. Astron. Soc.*, 425, 1215
- Knobel, C., Lilly, S. J., Iovino, A., et al. 2009, *Astrophys. J.*, 697, 1842
- Kormendy, J., & Ho, L. C. 2013, *Annu. Rev. Astron. Astrophys.*, 51, 511
- Koulouridis, E., Plionis, M., Melnyk, O., et al. 2014, *Astron. Astrophys.*, 567, 83
- Leauthaud, A., Finoguenov, A., Kneib, J-P, et al. 2010, *Astrophys. J.*, 709, 97
- Martini, P., Kelson, D. D., Kim, E., et al. 2006, *Astrophys. J.*, 644, 116
- Martini, P., Mulchaey, J. S., & Kelson, D. D. 2007, *Astrophys. J.*, 664, 761
- Martini, P., Sivakoff, G. R., Mulchaey, J. S. 2009, *Astrophys. J.*, 701, 66
- Martini, P., Miller, E. D., Brodwin, M., et al. 2013, *Astrophys. J.*, 768, 1
- Merloni, A., Rudnick, G., & Di Matteo, T. 2004, *Mon. Not. R. Astron. Soc.*, 354, L37
- Miller, C. J., Nichol, R. C., Gómez, P. L., Hopkins, A. M., & Bernardi, M. 2003, *Astrophys. J.*, 597, 142
- Miyaji, T., Krumpel, M., Coil, A. L., & Aceves, H. 2011, *Astrophys. J.*, 726, 83
- Oh, S., Mulchaey, J. S., Woo, J-H, et al. 2014, *Astrophys. J.*, 790, 43
- Peng, Y., Maiolino, R., & Cochrane, R. 2015, *Nature*, 521, 192
- Sanders, D. B., Soifer, B. T., Elias, J. H., et al. 1988, *Astrophys. J.*, 325, 74
- Serber, W., et al. 2006, *Astrophys. J.*, 643, 68
- Shen, Y., Mulchaey, J. S., Raychaudhury, S., Rasmussen, J., & Ponman, T. J. 2007, *Astrophys. J.*, 654, L115
- Silverman, J. D., Green, P. J., Barkhouse, W. A., et al. 2008, *Astrophys. J.*, 679, 118
- Silverman, J. D., Kovač, K., Knobel, C., et al. 2009, *Astrophys. J.*, 695, 171
- Simkin, S. M., Su, H. J., & Schwarz, M. P. 1980, *Astrophys. J.*, 237, 404
- Tomczak, A. R., Tran, K-V H., & Saintonge, A. 2011, *Astrophys. J.*, 738, 65
- Tremaine, S., Gebhardt, K., Bender, R., et al. 2002, *Astrophys. J.*, 574, 740
- Tzanavaris, P., Gallagher, S. C., Hornschemeier, A. E., et al. 2014, *Astrophys. J. Suppl. Ser.*, 212, 9
- Vijayaraghavan, R., & Ricker, P. M. 2015, *Mon. Not. R. Astron. Soc.*, 449, 2312
- Yang, Y., Mushotzky, R.F., Barger, A. J., & Cowie, L. L. 2006, *Astrophys. J.*, 465, 68

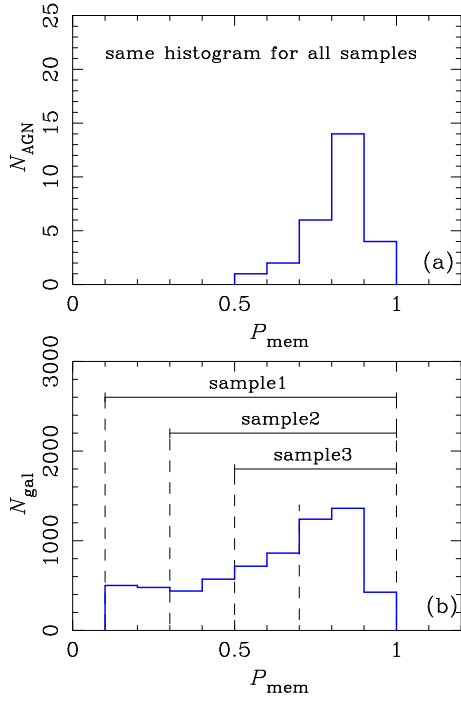


**Fig. 1** Distribution of membership probability ( $P_{\text{mem}}$ ) for 27 AGNs and 6,597 galaxies in groups with  $P_{\text{mem}} > 0.1$ .

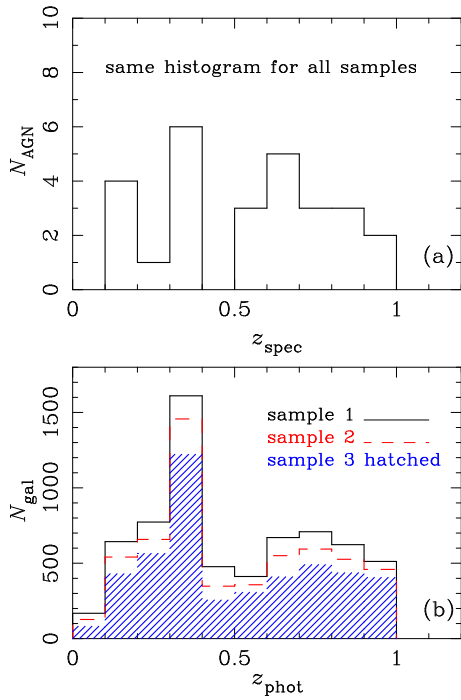


**Fig. 2** Redshift distributions of 27 AGNs and 6,597 galaxies in groups for three  $P_{\text{mem}}$  thresholds.

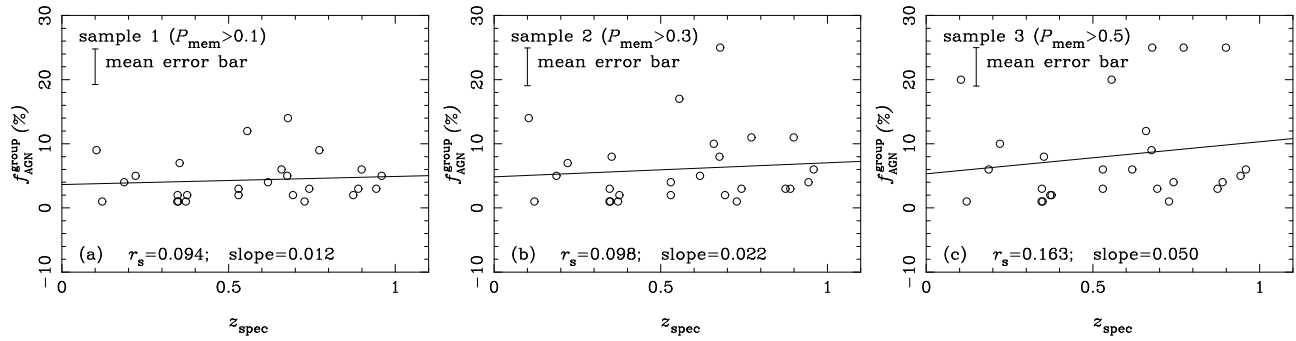


**Fig. 3** The AGN fraction versus as the AGN spectroscopic redshift for three samples of group galaxies. The solid line is the linear fit. The Spearman correlation coefficient ( $r_s$ ) and the slope of the best linear fit are presented in the bottom in each panel, as well as the mean error on the left corner.

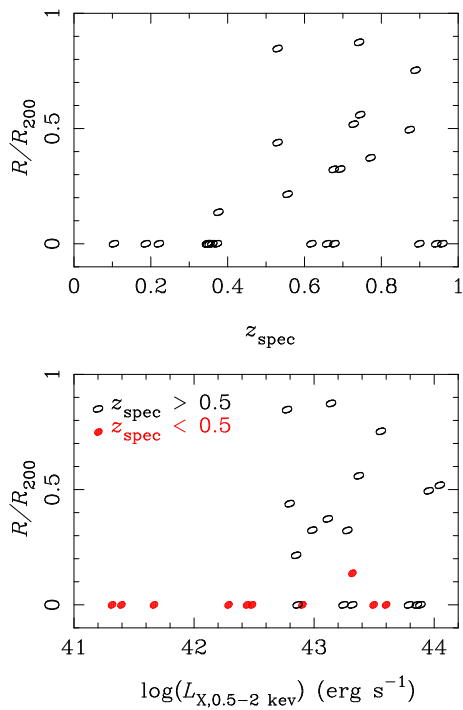


**Fig. 4** Distribution of normalized projected distance,  $R/R_{200}$ , for 27 AGNs as a function of spectroscopic redshift in groups (top) and the X-ray rest-frame luminosity in soft band (bottom).

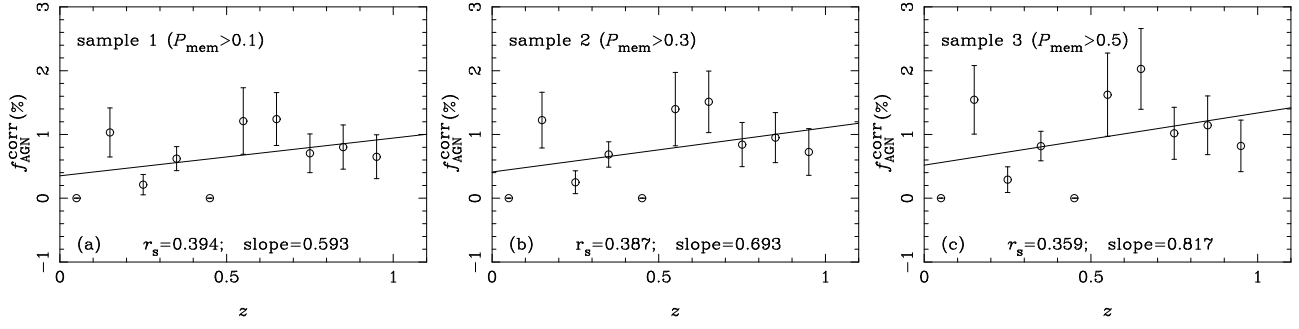


**Fig. 5** Overall AGN fraction versus the median redshift in 10  $z$ -bins for 198 X-ray selected galaxy groups. The solid line is the linear fit. The Spearman correlation coefficient ( $r_s$ ) and the slope of the best linear fit are presented in the bottom in each panel.

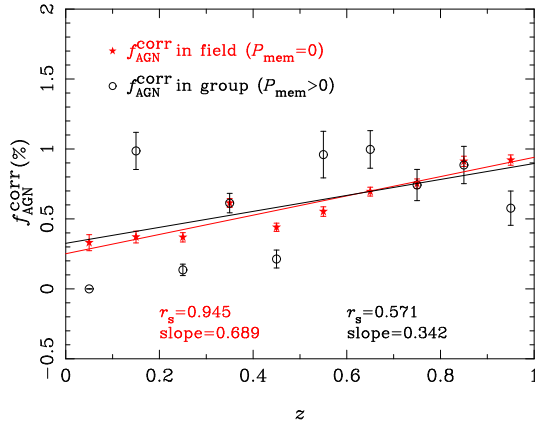


**Fig. 6** The AGN fraction as a function of redshift in groups ( $P_{\text{mem}} > 0$ , black circles) and fields ( $P_{\text{mem}} = 0$ , red stars). The solid lines are the best linear fits for the AGN fraction in groups (in black) and in fields (in red).

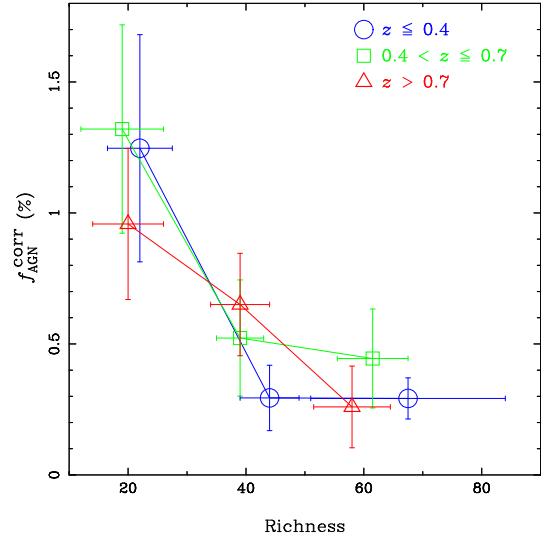


**Fig. 7** The corrected AGN fraction as a function of group richness. Blue circles, green rectangles and red triangles denote AGN fraction in  $z \leq 0.4$ ,  $0.4 < z \leq 0.7$  and  $z > 0.7$ , respectively. Error bars are the median absolute deviation from median in each bin.